International Journal of Applied Engineering Research ISSN 0973-4562 Volume 14, Number 12 (2019) pp. 2855-2860

Performance Evaluation of Wind Energy Conversion Systems Employing Space Vector Controlled Doubly-Fed Induction Generators

Dr.M.RaghavendraRao[1*], M.Ashraf Afrin[2]

[1]Electrical and Electronics Engineering Department,*
NOVA College of Engineering and Technology, Vegavaram– 534447, India.

[2]Electrical and Electronics Engineering Department,
NOVA College of Engineering and Technology, Vegavaram– 534447, India.

Abstract:

Nowadays world is suffering with the problem of increasing demand for electric power and global warming caused by emissions from industries used to meet this power demand. In countries where per capita power consumption is minimum, there is requirement for continuous power capacity addition without affecting the environment. A wind energy conversion system (WECS) is perfect solution to those two problems. Variable speed wind energy conversion system is able to convert the varying incoming wind power as rotational energy, by changing the speed of the wind turbine. The doubly-fed induction generators (DFIG) are widely used in WECS using back to back converters. Indeed, amongst many variable speed concepts, WECS using DFIG have many advantages over others. It is essential to conduct fault studies in a power system consisting of distributed generation (DG), in particular if it consists of WECS connected to grid by a line. A fault occurring on this line severely effects the operation of back to back PWM converters and DFIG. In this paper simulation studies are carried out to identify the effects of instantaneous and gradual variation of wind speeds and various types of faults in line section on the operation of WECS employing space vector controlled DFIG.

Keywords: Wind energy conversion systems, Doubly-fed induction generator, Wind speed, Pitch angle; Active power; Reactive power.

INTRODUCTION

World is facing two major problems, increasing demand for electric power and global warming caused by emissions from different industries. Continuous power capacity addition with minimum impact on environment is the need of the hour. In developing economies, the bulk of the electric power has been generated by conventional ways. Hence priority is given to generating electrical power with innovative methods, making sure that these innovations are not destructive to the environment. Wind energy conversion systems (WECS) gained prominence over the years because of generation of electrical power with no emissions. With improved technologies the cost of wind power has reduced to about one sixth of the cost two decades ago [1]. Fixed speed and variable speed turbines are two types of turbines used for WECS. Aerodynamic control is essential for better performance of the system with a fixed speed WECS. This leads to complexities in system with increased controls and costs. Variable speed turbine systems change the speed of the wind turbine to convert varying incoming wind power as rotational energy. This leads to smoother electrical power with reduced stress on the mechanical structure. Maximum power point tracking technique (MPPT) is used to control the electrical power developed to its maximum value [2]. WECS employing doubly-fed induction generators (DFIG) use back to back pulse width modulated (PWM) converters as shown in Fig.1.

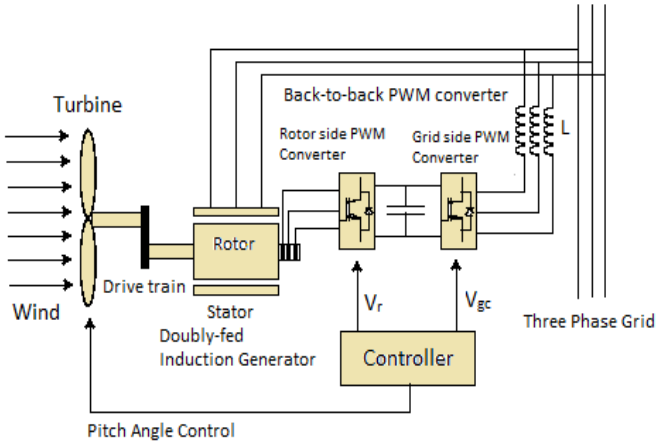

Figure 1. Schematic diagram of DFIG

The back to back PWM converter consists of two converters, the rotor side converter and grid side converter. These rotor side and grid side converters are controlled independently of each other. Grid side converter controls the voltage. Rotor side converter transfers power in and out of the rotor depending on the operating condition of the drive. Power flows from the rotor to grid in over-synchronous situation, whereas it flows from grid to rotor in sub-synchronous situation. In both situations the stator supplies power to the grid.

WECS employing back to back converters in DFIG have many advantages over other variable speed turbine systems. These converters carry only the rotor power which is nearly

20% of the total machine power [3]-[4]. Therefore rating of the converter used in DFIG can be kept very low as compared to the series converters used in other generators which carry total machine power. Reactive power management is another important aspect in WECS. The arrangement of converters in DFIG improves reactive power control as in the case of synchronous generators, and is more economical for variable speed operation [5]-[8].

Fault studies play an important role in power system analysis. It is essential to conduct fault studies in a power system consisting of distributed generation (DG), in particular if DG consists of WECS. A fault occurring on the line connecting wind farm to grid severely effects the operation of DFIG. Fault studies are required to identify appropriate relay settings and coordination among relays for backup protection. For selection and setting up of ground relays and phase relays line to ground fault and three phase fault analyses are essential [9].

MATHEMATICAL MODELING:

DFIG dynamic model is essential to develop decoupled control of active and reactive power. The DFIG consists of three phase stator winding and a three phase rotor winding similar to a wound rotor induction machine. Slip rings are used to feed three phase rotor winding. In a stationary reference frame the voltage and torque equations of the DFIG are given by

$$v_{sj} = r_s \,.\, i_{sj} + \frac{\partial \psi_{sj}}{\partial t} \tag{1}$$

$$v_{Rj}{}' = r_R{}' \,.\, i_{Rj}{}' + \frac{\partial \psi_{Rj}}{\partial t} \tag{2}$$

$$T_{el} = \frac{p}{2} \,.\, \sum_{j=1}^{3} i_j . \frac{\partial \psi_j}{\partial \vartheta} \tag{3}$$

The rotor voltage, current and resistance in these equations are referred to the stator. Superscript notation is used for transformed rotor quantities. The synchronous reference frame (dq) equations are obtained by transforming the above three phase equations to two phase components.

$$v_d = \frac{2}{3}\left[v_1 . cos\vartheta + v_2 . \cos\left(\vartheta - \frac{2.\pi}{3}\right) + v_3 . \cos\left(\vartheta + \frac{2.\pi}{3}\right)\right] \tag{4}$$

$$v_q = \frac{2}{3}\left[v_1 . cos\vartheta + v_2 . \cos\left(\vartheta - \frac{2.\pi}{3}\right) + v_3 . \cos\left(\vartheta + \frac{2.\pi}{3}\right)\right] \tag{5}$$

$$\bar{v} = v_d + j . v_q \tag{6}$$

$$\bar{v_s} = r_s . \bar{\imath_s} + \frac{\partial \bar{\psi}_s}{\partial t} + j . \omega_s . \bar{\psi}_s \tag{7}$$

$$\bar{v_r}' = r_R' . \bar{\imath}_R' + \frac{\partial \bar{\psi}_R'}{\partial t} + j . \omega_R . \bar{\psi}_R' \tag{8}$$

$$\bar{\psi}_s = L_s . \bar{\imath_s} + L_m . \bar{\imath}_R' \tag{9}$$

$$\bar{\psi}_R = L_m . \bar{\imath_s} + L_R . \bar{\imath}_R' \tag{10}$$

$$T_{el} = \frac{3}{2} \,.\, p . Im\{\bar{\psi}_s . \vec{\imath}_s^*\} \tag{11}$$

DFIG works as a generator with constant stator voltage, hence a reference frame related to the stator voltage space vector is a suitable option [10]. Selection of state variables plays an important role in the development of DFIG dynamic equations. Induction machine model will be developed if the air-gap flux is selected as state variable. Whereas selecting rotor flux linkage as state variable leads to a synchronous machine model. However both of these models provide useful information on DFIG working and controlling aspects [11]-[13]. Neglecting stator resistance the stator voltage (7) can be represented under steady state as

$$\bar{V_s} = j . \omega_s . L_s \bar{I_s} + \bar{V_b} \tag{12}$$

$$\bar{V_b} = j . \omega_s . L_m \bar{I_R'} \tag{13}$$

The rotor current induces a back emf in stator and is represented in (13). This current can be treated as the synchronous DFIG field current. The approximate rotor voltage magnitude is given in (14) after neglecting resistance and leakage inductance of rotor.

$$V_R \approx s * a_{SR} * V_s \tag{14}$$

In (14) a_{SR} represents the stator to rotor voltage transformation ratio. The slip of the machine s is given in (15).

$$s = \frac{\omega_s - \omega_{mech}}{\omega_s} = \frac{\omega_R}{\omega_s} \tag{15}$$

Active power delivered to the rotor by converter is represented in (16). The mechanical power delivered to the shaft of the generator is given in (17).

$$P_R = s * P_s \tag{16}$$

$$P_{mech} = (1 - s) * P_s \tag{17}$$

Under both over-synchronous and sub-synchronous speed conditions the power flow in the DFIG can be found from (16) and (17). For over-synchronous speeds, the converter works as generator of active power transferring power to the grid. For sub-synchronous speeds, the converter by-passes power from the grid into the rotor circuit. Based on the dynamic equations represented above, a feed forward controller block diagram is represented in Fig.2. Normally stator or rotor flux vectors are used in drives controllers. But stator voltage space vector is used in the present model making it a vector controller. All stator and rotor currents are transformed into the synchronous reference frame. A decoupling circuit calculates the required active and reactive power signals from rotor voltage.

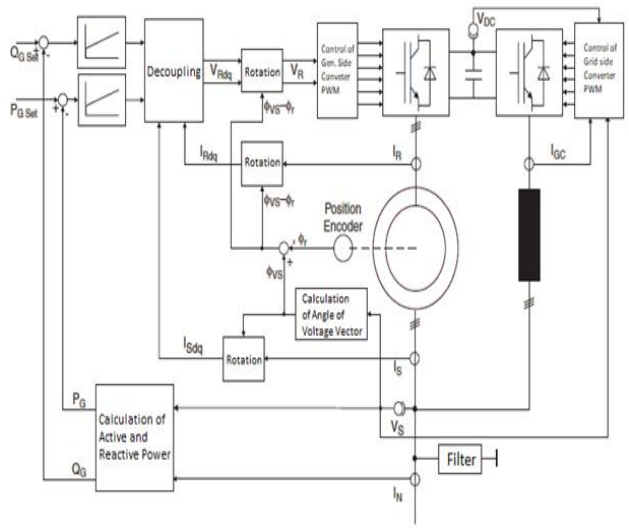

Figure 2. DFIG vector controller block diagram

SIMULATION

A physical model of the WECS with space vector controlled DFIG connected to grid by a line is created in simulink. The stator windings of DFIG are directly connected to the 50 Hz grid while the rotor windings are fed at variable frequency through the back to back PWM converters through slip rings. WECS consists of six 1.5 MW, 50 Hz wind turbines connected to 120kV grid by a 30 km length 25kV line. A combined 2 MVA induction motor load and 200 kW resistance load are connected at the middle of transmission line connecting wind farm to grid as shown in Fig.3.

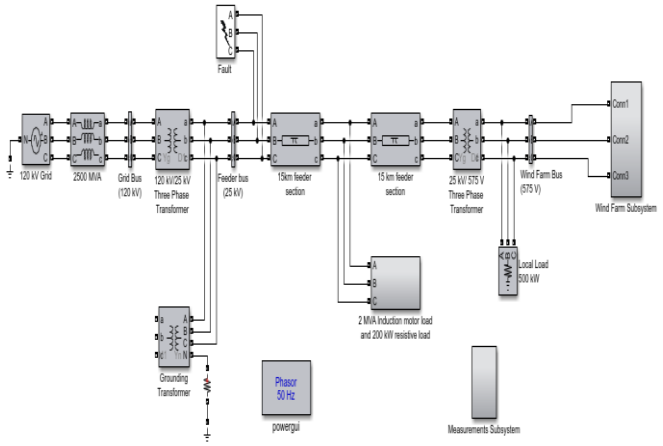

Figure 3. Simulation diagram

The presented model is simulated and analyzed using simulink in two different scenarios. These Scenarios are (i) Instantaneous variation of wind speed from 8 m/s to 16 m/s at t=0 sec. (ii) Gradual variation of wind speed from 8 m/s to 16 m/s at a rate of 1m/s^2 from t=0 sec, and single line to ground fault on transmission line connecting wind farm to grid at location shown in Fig.3 at 20 sec. In all these scenarios it is assumed that the initial wind speed is 8 m/s, pitch angle (θ) of blades is 0^o, angular speed of wind turbine (ω) is 0.8 pu, and active power generated by wind farm is 1.87 MW and reactive power consumption is 0.093 Mvar.

RESULTS AND DISCUSSION

Scenario (i)

Table 1 and Figure 4 show the variation of turbine speed (ω), pitch angle of blades (θ), wind farm bus voltage (V_{wf}) and wind farm current (I_{wf}) with instantaneous variation of wind speed from 8 m/s to 16 m/s at t=0 sec. It is observed that ω starts increasing from 0.8 pu at 0 sec to a value of 1.227 pu at 10.735 sec corresponding to the sudden increase in wind speed. From 8.966 sec onwards θ starts to increase to control ω. At 12.319 sec, θ reached to its peak vale of 6.773^o and finally settled at a value of 2.922^o nearly at 20 sec. By that time ω remained constant at 1.216 pu. This is an expected behavior of the pitch angle controller to maintain turbine speed constant corresponding to the increase in mechanical power, with minimum stress on the mechanical structure of wind turbine. The wind farm bus voltage almost all remained constant at a value of 1 pu with increased current from 0.187 pu to 0.881 pu to generate active power near its settling value of 8.782 MW.

Table 1 Variation of ω, θ, Vwf AND Iwf with instantaneous change in wind speed from 8 m/s to 16 m/s at 0 sec.

t (sec)	ω (pu)	θ (deg)	V_{wf} (pu)	I_{wf} (pu)
0	0.8	0	1	0.187
5	1.015	0	1.001	0.388
8.966	1.211	0.067	1.002	0.885
10	1.226	2.136	1.002	0.881
10.735	1.227	3.606	1.002	0.881
12.319	1.224	6.773	1.002	0.881
15	1.217	3.750	1.002	0.881
20	1.216	2.922	1.002	0.881

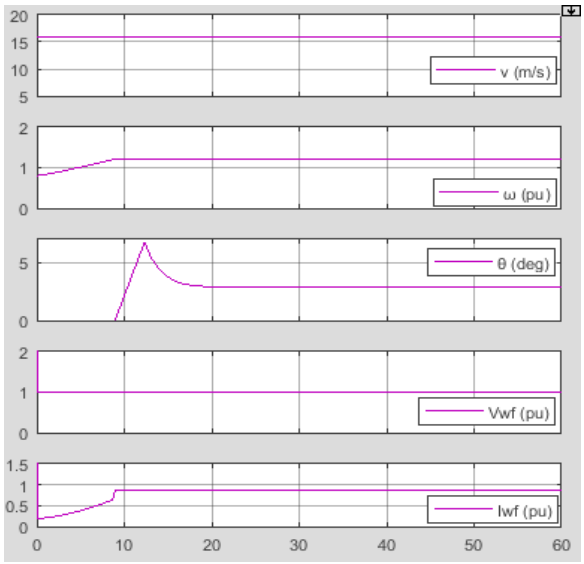

Fig. 4 - Variation of Variation of ω, θ, V_{wf} and I_{wf} with instantaneous change in wind speed from 8 m/s to 16 m/s at 0 sec.

Table 2 and figure 5 show the variation of wind farm active power (P_{wf}) and reactive power (Q_{wf}), transmission line connecting wind farm with grid active power (P_{fr}) and reactive power (Q_{fr}) flows with instantaneous change in wind speed from 8 m/s to 16 m/s at t=0 sec. Initially wind farm is generating an active power of 1.870 MW and a reactive power of -0.093 Mvar (-ve sign indicates that wind farm consumes reactive power). Line connecting wind farm with grid draws an active power of 0.551 MW and reactive power of +0.003 Mvar from grid (+ve sign indicates that power flow is from grid to wind farm). From table 2 and figure 5 it is observed that from 0 sec onwards generated power from wind farm increased with respect to time and reached to a peak value of 8.819 MW at 8.966 sec and settled at a value of 8.782 MW. Consequently the reactive power consumption also increased with respect to time reaching a peak value of 0.962 Mvar at 8.966 sec and settled at a value of 0.944 Mvar. It is evident from table 2 and figure 5 that line draws both active power and reactive power from grid and supplies active power to load connected at the middle of the line section and reactive power to the wind farm. The active power taken by line from grid gradually decreased to 0 MW at 1.890 sec and settled at a value of -6.051 MW (-ve sign indicates active power flow is from wind farm to grid) but reactive power taken from grid increased from 0.003 Mvar to 1.999 Mvar. This behavior is expected since active power generation of wind farm increased to 8.782 MW with increased reactive power consumption up to 0.944 Mvar.

Table 2 Variation of Pwf, Qwf, Pfr and Qfr with instantaneous change in wind speed from 8 m/s to 16 m/s at 0 sec.

t (sec)	P_{wf} (MW)	Q_{wf} (Mvar)	P_{fr} (MW)	Q_{fr} (Mvar)
0	1.870	-0.093	0.551	0.003
1.890	2.425	-0.202	0	0.132
5	3.847	-0.450	-1.393	0.490
8.966	8.819	-0.962	-6.092	2.027
10	8.781	-0.943	-6.050	1.999
15	8.782	-0.944	-6.051	1.999
20	8.782	-0.944	-6.051	1.999

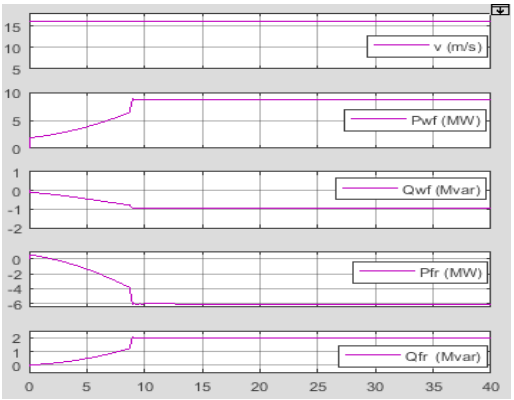

Fig. 5 - Variation of P_{wf}, Q_{wf}, P_{fr} and Q_{fr} with instantaneous change in wind speed from 8 m/s to 16 m/s at 0 sec

Scenario (ii)

Table 3 and figure 6 show the variation of ω, θ, V_{wf} and I_{wf} with gradual change in wind speed from 8 m/s to 16 m/s at a rate of 1 m/s^2 and occurrence of a single line to ground fault at 20 sec on line section.

During pre-fault period (t < 20 sec) it is observed that ω increased from 0.8 pu to 1.227 pu in 13.685 sec. From 11.91 sec onwards θ started to increase to control ω. θ reached to a peak vale of 6.787^o at 15.276 sec and settled at a value of 3.119^o nearly at 20 sec, by that time turbine speed remained constant at 1.216 pu. This is an expected behavior of the pitch angle controller to maintain turbine speed constant corresponding to the increase in mechanical power with minimum stress on the mechanical structure of wind turbine.

Occurrence of single line to ground fault at 20 sec caused a dip in wind farm voltage from 1.002 pu to 0.902 pu, but regained to a value of 1 pu at 20.048 sec. This momentary variation of 0.1 pu in voltage is not sustained for duration of 0.1 sec, which is the setting of under voltage relay and wind farm protection system is not tripped. Consequently during the voltage dip period, current from wind farm increased from 0.881 pu to 0.959 pu to maintain generated power of 8.782 MW.

It is evident from table 3 and figure 6 that single line to ground fault has no effect on angular velocity of turbine (ω). It is due to the fact that fault is cleared in nine cycles and has no effect on rotating system having relatively large time constant.

Table 3 Variation of ω, θ, Vwf and Iwf with gradual change in wind speed from 8 m/s to 16 m/s at a rate of 1 m/s^2 from 0 sec. Single line to ground fault at 20 sec.

t (sec)	ω (pu)	θ (deg)	V_{wf} (pu)	I_{wf} (pu)
0	0.8	0	1	0.187
5	0.892	0	1	0.261
10	1.119	0	1.001	0.520
11.91	1.211	0.056	1.001	0.885
13.685	1.227	3.606	1.002	0.881
15	1.225	6.236	1.002	0.881
15.276	1.224	6.787	1.002	0.881
20	1.216	3.119	1.002	0.881
20.017	1.216	3.117	0.902	0.959
20.044	1.217	3.171	0.991	0.668
20.048	1.217	3.179	1.000	0.652
21.091	1.221	5.265	1.002	0.881
25	1.216	3.111	1.002	0.881
30	1.216	2.901	1.002	0.881
35	1.216	2.896	1.002	0.881
40	1.216	2.896	1.002	0.881

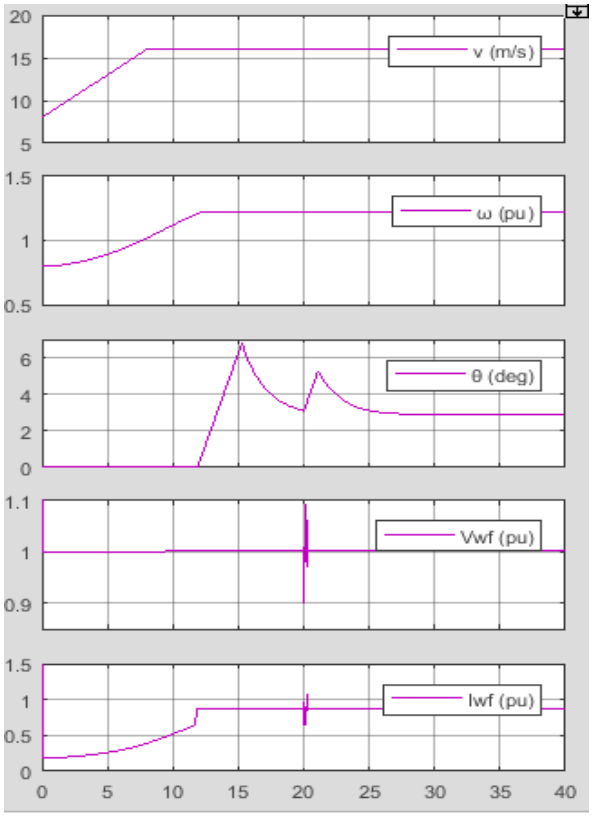

Fig. 6 - Variation of Variation of ω, θ, V_{wf} and I_{wf} with gradual change in wind speed from 8 m/s to 16 m/s at a rate of 1 m/s^2 from 0 sec. Single line to ground fault at 20 sec.

Table 4 and figure 7 show the variation of P_{wf}, Q_{wf}, P_{fr} and Q_{fr} with gradual change in wind speed from 8 m/s to 16 m/s at a rate of 1 m/s^2 and occurrence of a single line to ground fault at 20 sec on line section. It is observed that generated power of wind farm increased from 1.870 MW to a peak value of 8.815 MW at 11.91 sec and settled at a value of 8.782 MW.

Table 4 Variation of P_{wf}, Q_{wf}, P_{fr} and Q_{fr} with gradual change in wind speed from 8 m/s to 16 m/s at a rate of 1 m/s^{2}from 0 sec. Single line to ground fault at 20 sec.

t (sec)	P_{wf} (MW)	Q_{wf} (Mvar)	P_{fr} (MW)	Q_{fr} (Mvar)
0	1.870	-0.093	0.551	0.003
4.351	2.426	-0.202	0	0.133
5	2.605	-0.236	-0.177	0.176
10	5.169	-0.638	-2.667	0.854
11.91	8.815	-0.966	-6.084	2.028
15	8.780	-0.944	-6.050	1.999
20	8.782	-0.944	-6.051	1.999
21.091	8.781	-0.943	-6.048	1.999
25	8.782	-0.944	-6.051	1.999
30	8.782	-0.944	-6.051	1.999
35	8.782	-0.944	-6.051	1.999
40	8.782	-0.944	-6.051	1.999

Consequently the reactive power consumption also increased to a peak value of 0.966 Mvar at 11.91 sec and settled at a value of 0.944 Mvar. The active power taken by line from grid gradually decreased to 0 MW at 4.351 sec and settled at a value of -6.051 MW but reactive power taken from grid increased from 0.003 Mvar to 1.999 Mvar. This is an expected behavior since active power generation from wind farm increased to 8.782 MW with increased reactive power consumption up to 0.944 Mvar. It is observed that steady state pre fault powers in scenario (ii) are matching with corresponding values in scenario (i). At 20 sec single line to ground fault occurred at the grid side of line and continued to maintain pre-fault powers as wind farm is not tripped.

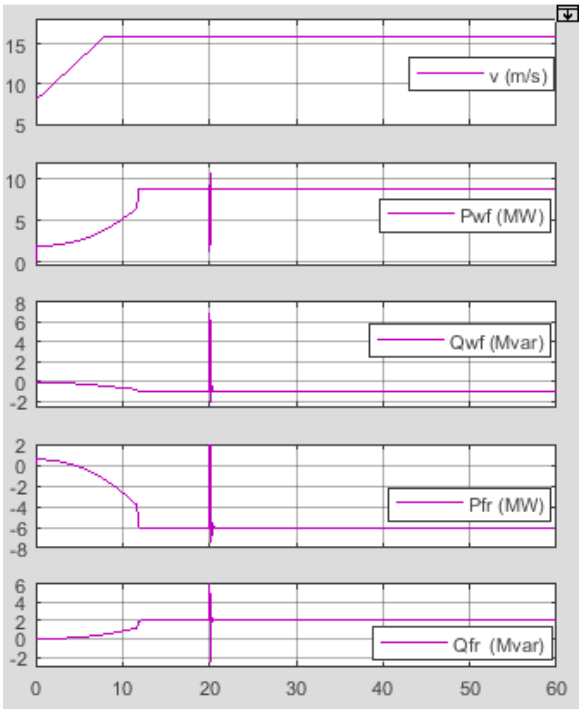

Fig. 7 - Variation of P_{wf}, Q_{wf}, P_{fr} and Q_{fr} with gradual change in wind speed from 8 m/s to 16 m/s at a rate of 1 m/s^2 from 0 sec. Single line to ground fault at 20 sec.

CONCLUSIONS

A model has been formulated to simulate the performance of wind farm employing space vector controlled doubly-fed induction generators. The effects of instantaneous and gradual variation of wind speed and occurrence of a single line to ground fault on a transmission line connecting wind farm with grid has been presented and analyzed. The results show that the pitch angle controller effectively controlled the turbine speeds with increase in mechanical power because of instantaneous and gradual increase in wind speeds. A single line to ground fault on line connecting wind farm with grid has not affected the operation of wind farm as angular velocity of turbine remained constant and fault is cleared in nine cycles. Pitch angle controller effectively controlled angular speed to within safe limits by adjusting pitch angle of blades. Space vector controlled doubly-fed induction

generator in conjunction with turbine pitch angle controller showed excellent response irrespective of wind speed variations and single line to ground fault.

ACKNOWLEDGEMENTS

The authors are thankful to correspondent Dr.Vijaya Nirmala Muttamsetty and Secretary Ln. Krishna Rao Muttamsetty of NOVA College of Engineering and Technology, Vegavaram for their encouragement and support to publish this work.

REFERENCES

[1] Ackermann, T., 2005, "Wind Power in Power Systems" John Wiley & Sons Ltd.

[2] Koutroulis, E., and Kalaitzakis, K., 2006, "Design of a maximum power tracking system for Wind energy conversion applications," IEEE Trans. industrial Electronics, vol.53, no.2, pp. 486-494.

[3] Carlin, P., Laxson, A., and Muljadi, E., 2001 "The History and state of the art of variable- speed wind turbine technology," NREL Technical Report, TP-500-28607.

[4] Amirat, Y., Benbouzid, M., Bensaker, B., and Wamkeue, R., 2007, "Generators for Wind Energy Conversion Systems: State of the Art and Coming Attractions, Journal of Electrical Systems, vol.3, no 1, pp. 26-38.

[5] Muller, S., Deicke, M., and DeDoncker, R., 2002, "Doubly fed induction generator systems for wind turbines," IEEE Industry Applications Magazine, vol. 8, no 3, pp. 26-33.

[6] Datta, R., and Ranganathan, V., 2002, "Variable-speed wind power generation using doubly fed wound rotor induction machine – A comparison with alternative schemes," IEEE Trans. Energy Conversion, vol. 17, no 3, pp. 414-421.

[7] Holdsworth, L., Wu, X., Ekanayake, J., and Jenkins, N., 2003, "Comparison of fixed speed and doubly-fed induction wind turbines during power system disturbances," IEE Proc. Generation, Transmission and Distribution, vol. 150, no 3, pp. 343-352.

[8] Grabic, S., and Katic, V., 2004, "A comparison and trade-offs between induction generator control options for variable speed wind turbine applications," Proceedings of IEEE International Conference on Industrial Technology (ICIT), vol. 1, Hammamet (Tunisia), pp. 564-568.

[9] Saadat, H., 1999, "Power Systems Analysis" WCB McGraw-Hill.

[10] Jahns, T., and DeDoncker, R., 1996, "Control of generators," The Control Handbook, Boca Raton, FL: CRC.

[11] Pena, R., Clare, J., and Asher, G., 1996, "Doubly fed induction generator using back-to-Back PWM converters and its application to variable-speed wind-energy generation," IEE Proc.- Electr. Power Appl., Vol. 143, No. 3, pp. 231-241.

[12] Akhmatov, V., 2002, "Variable- Speed Wind Turbines with Doubly- Fed Induction Generators, Part I: Modelling in Dynamic Simulation Tools," Wind Engineering Volume 26, No. 2, pp. 85-108.

[13] Nicholas, W., Sanchez-Gasca, J., William, P., and Robert, D., 2003, "Dynamic modeling of GE 1.5 and 3.6 MW wind turbine-generators for stability simulations," GE Power Systems Energy Consulting, IEEE WTG Modeling Panel, pp. 1977- 1983.

BIOGRAPHY

Dr.RaghavendraRao Maarisetti received the B.Tech. from V.R.Siddhartha Engineering College, of the Nagarjuna University, the M.Tech from the JNTUniversity College of Engineering, Hyderabad, and the Ph.D from the JNTUniversity Kakinada, all in Electrical and Electronics Engineering. Currently he is Professor of Electrical and Electronics Engineering Department and Principal of NOVA College of Engineering and Technology, Vegavaram, India. His primary areas of interest include power system design, modeling and alternative energy resources. Dr.Maarisetti is a Fellow of Institute of Engineers (FIE) India and a chartered engineer (CE), life member of Indian Society for Technical Education (LMISTE) and a member of Institute of Electrical and Electronics Engineers (MIEEE).

Ashraf Afrin Mohammad received the B.Tech. in Electrical and Electronics Engineering from Rajamahendri Institute of Engineering and Technology, of the JNTUniversity Kakinada in 2017. She is now pursuing the M.Tech in Electrical and Electronics Engineering from the NOVA College of Engineering and Technology, Vegavaram, India. Her areas of interest include power system design, modeling and renewable energy resources.